J|A|C|S COMMUNICATIONS

Published on Web 09/22/2009

Efficient Near-IR Hyperthermia and Intense Nonlinear Optical Imaging Contrast on the Gold Nanorod-in-Shell Nanostructures

Kuo-Wei Hu,[†] Tzu-Ming Liu,[‡] Kuei-Yi Chung,[†] Keng-Shiang Huang,[§] Chien-Tai Hsieh,[‡] Chi-Kuang Sun,[||] and Chen-Sheng Yeh*,[†]

Department of Chemistry and Center for Frontier Materials and Micro/Nano Science and Technology, National Cheng Kung University, Tainan 701, Taiwan, Institute of Biomedical Engineering, National Taiwan University, Taipei 106, Taiwan, Department of Biomedical Engineering, I-Shou University, Kaohsiung County 840, Taiwan, and Department of Electrical Engineering and Graduate Institute of Photonics and Optoelectronics, National Taiwan University, Taipei 106, Taiwan

Received July 27, 2009; E-mail: csyeh@mail.ncku.edu.tw

Gold nanorods (Au NRs) simultaneously act as near-IR (NIR) hyperthermia and nonlinear optical imaging agents, an important property for nanobiotechnology. Au NRs with a strong surface plasmon resonance (SPR) in the NIR region have shown their potential in photoinduced therapeutic applications.[1] For noninvasive therapy, NIR radiation is used because it penetrates tissue more deeply but is absorbed less than other types of radiation. Additionally, the SPR of Au NRs can locally augment the field of incident electromagnetic waves, increasing the yield of nonlinear optical processes. Thus, Au NRs are ideally suited for use as nonlinear optical contrast agents in cell imaging using two-photon-excited luminescence.[2] It is always highly desired to develop metal nanomaterials with a strong SPR response upon photoexcitation. To preserve the NIR absorption, biocompatibility, and easy surface modification, new Au NR-in-shell nanostructures, inspired by Au@Ag (core/shell) NRs having greater SPR strength,[3] were developed to be more efficacious than Au NRs in NIR hyperthermia and nonlinear optical imaging contrast. With their extraordinarily broad and strong SPR band, Au NR-in-shell nanostructures efficiently augmented several multiphoton nonlinear processes accompanied by strong multiphoton fluorescence, 55 times larger than that of Au NRs.

A seedless method[4] was used to prepare Au NRs with an aspect ratio of ~3.9 (length 38.2 nm, width 9.8 nm) (Figure 1a). Subsequently, a Ag nanolayer was formed on the Au NRs via reactions of $AgNO_3$ and ascorbic acid using a modified version of a previously published method.[3a] Figure 1b shows the morphology of the resulting Au@Ag nanorods, with some nanorods exhibiting a clear differential contrast from the darkened Au nanorods embedded in the Ag nanolayer. The thickness of the Ag nanolayer could be varied by changing the amount of $AgNO_3$ and was estimated to be 4−5 nm in the present study (Figure 1b). Our previous studies showed that transforming Ag into Au/Ag nanostructures significantly decreased the toxicity of Ag.[5] Thus, Au@Ag nanorods were allowed to react with $HAuCl_4$ aqueous solution, which yielded Au NR-in-shell nanostructures via a replacement reaction. Intact Au NRs were embedded in hollow Au/Ag shells with a shell thickness of ~4.8 nm (Figure 1c). The shell thickness could be tuned by changing the amount of $HAuCl_4$ (see Figure S1 in the Supporting Information). High-resolution transmission electron microscopy (HRTEM) indicated the single crystalline nature of the Au/Ag nanoshell with a lattice spacing of 0.238 nm (Figure 1c, inset). Energy-dispersive X-ray (EDX) analysis of single Au NR-in-shell nanostructures indicated an alloy structure with an average Au/Ag atomic ratio of 47:53 (Figure S2). A line-scan EDX evaluation was further performed to measure the transverse and axial directions of a single Au NR-in-shell nanostructure (Figure S3). Each profile revealed the compositions of Au and Ag, with a dominant Au component in the middle part of the nanostructure where the Au NR is located within the shell. The Au NR-in-shell nanostructures were dispersed in H_2O and appeared as a blue colloidal solution. Figure 1d shows the extinction spectra of as-prepared Au NRs and Au NR-in-shell nanostructures, both measured with 8.7×10^{10} particles/mL. The Au NR longitudinal SPR peaked at ~800 nm, and the transverse SPR band was centered at 520 nm; the Au NR-in-shell nanostructures had a broad band from ~400 to ~1100 nm, with the maximum at ~900 nm. The optical intensity of Au NR-in-shell nanostructures was much stronger than that of the Au NRs. Notably, the Au@Ag nanorods showed no apparent absorption in the NIR region and displayed poor temperature elevation upon irradiation with an NIR laser (Figure S4).

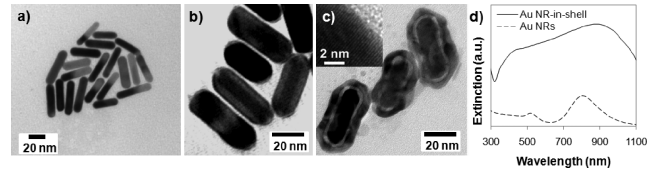

Figure 1. TEM images of (a) Au NRs, (b) Au@Ag nanorods, and (c) Au NR-in-shell nanostructures. The inset shows an HRTEM image of an Au/Ag nanoshell. (d) Extinction spectra of Au NRs and the Au NR-in-shell nanostructures, both measured with 8.7×10^{10} particles/mL.

Because of the toxic coating of cetyltrimethylammonium bromide (CTAB) molecules on the surface of the Au NRs, the Au NRs were modified using negatively charged poly-4-styrenesulfonic acid (PSS) and a subsequent deposition of positively charged polyethyleneimine (PEI).[5] The Au NR-in-shell nanostructures with a surface charge of +26 mV followed the same deposition sequence (PSS then PEI) to form PEI/PSS/Au NR-in-shell nanostructures. There was no obvious decrease in cell viability in cells containing surface-modified Au NR-in-shell nanostructures; however, cells containing the unmodified Au NR-in-shell nanostructures showed dose-dependent toxicity (Figure S5).

In the in vitro NIR hyperthermia experiments, the PEI/PSS-modified Au NRs and Au NR-in-shell nanostructures were conjugated with anti-EGFR for specific targeting of the A549 cells overexpressing epidermal growth factor receptor (EGFR).[1a,5] The cancer cells were treated with equal amounts (8.7×10^{10} particles/mL) of Au NRs and Au NR-in-shell nanostructures. The targeted cells were irradiated using an 808 nm continuous-wave (CW) laser. Cell damage caused by Au NRs was observable at 18 W cm^{-2} but not at 9 W cm^{-2} (Figure 2). On the

[†] National Cheng Kung University.
[‡] Institute of Biomedical Engineering, National Taiwan University.
[§] I-Shou University.
[||] Department of Electrical Engineering and Graduate Institute of Photonics and Optoelectronics, National Taiwan University.

10.1021/ja9062772 CCC: $40.75

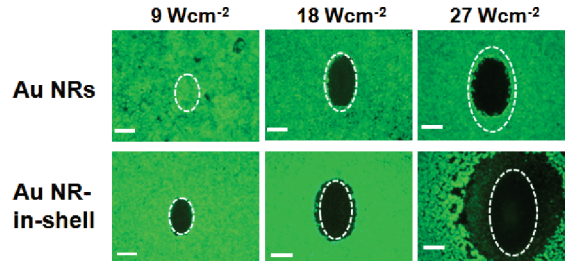

Figure 2. A549 cancer cells treated with anti-EGFR-conjugated Au NRs and Au NR-in-shell nanostructures were irradiated using an NIR CW laser at 9, 18, and 27 W cm^{-2} for 8 min of exposure at a particle concentration of 8.7×10^{10} particles/mL. The dotted circles indicate the laser beam area. The green fluorescence of calcein-AM indicates living cells. The scale bars correspond to 500 μm.

other hand, Au NR-in-shell nanostructures destroyed malignant cells at the half the laser power needed for Au NRs. After careful inspection, we found that the area of cells damaged by the Au NR-in-shell nanostructures was larger than the laser beam spot, while the area damaged by the Au NRs was limited to the area of the irradiation spot. We did additional experiments to examine whether NIR laser irradiation caused Ag ions to leak, thereby inducing toxicity and leading to a larger area of damaged cells. Au NR-in-shell nanostructure colloidal solutions were either exposed or not exposed to NIR laser irradiation. The supernatants were collected and analyzed using an ICP spectrometer to determine the amount of Ag^+ ions in the supernatants. We found no apparent increase (<2%) of Ag^+ after laser irradiation (Figure S6). These results indicated that the Au NR-in-shell nanostructures remained stable during NIR laser exposure. Although we cannot give a reasonable interpretation of how or why the Au NR-in-shell nanostructures caused damage beyond the laser beam size at this stage, one possibility may be the incorporation of Ag into the Au NR-in-shell nanostructure. Silver has greater thermal conductivity than gold. The thermal conductivity for bulk Ag (429 W m^{-1} K^{-1}) is larger than that for bulk Au (318 W m^{-1} K^{-1}).[6] After NIR laser irradiation, the heat generated by the Au NR-in-shell nanostructures readily flew to nanoparticles adjacent to the irradiated area, facilitated by the higher thermal conductivity of Ag, in turn increasing the hyperthermia efficiency.

The nonlinear optical properties of Au NRs and Au NR-in-shell nanostructures in their emission spectra and in vitro nonlinear microscopy imaging in A549 cancer cells were conducted using a home-built femtosecond (~100 fs) Cr:forsterite laser. The operating wavelength, 1230 nm, is in the biological penetration window and was used to perform in vivo submicrometer 3D section images with a large penetration depth.[7] The concentration of each particle used in the emission measurements was $\sim 10^9$ particles/mL. The measured emission spectra (60 s integration time; Figure S7) show that the Au NR-in-shell nanostructures generated multiphoton signals: second-harmonic generation (SHG) (sharp peak at ~615 nm), third-harmonic generation (THG) (sharp peak at ~410 nm), and multiphoton fluorescence signals (broad emission band) including four-photon fluorescence (4PF; emission band >308 nm). Such multiresonant augmentation resulted in an ultrabroadband fluorescence from ~390 nm to the NIR region. On average, the yield of the multiphoton signals of the Au NR-in-shell nanostructures was 55 times on average larger than that of the Au NRs. Multiphoton-induced images of A549 cancer cells treated with anti-EGFR-conjugated Au NRs and Au NR-in-shell nanostructures were taken in a multiphoton nonlinear microscope system (Figure 3). With the same voltage (1100 V) applied in the photomultiplier tube, the 3PF (yellow), SHG band (green), 2PF (red),

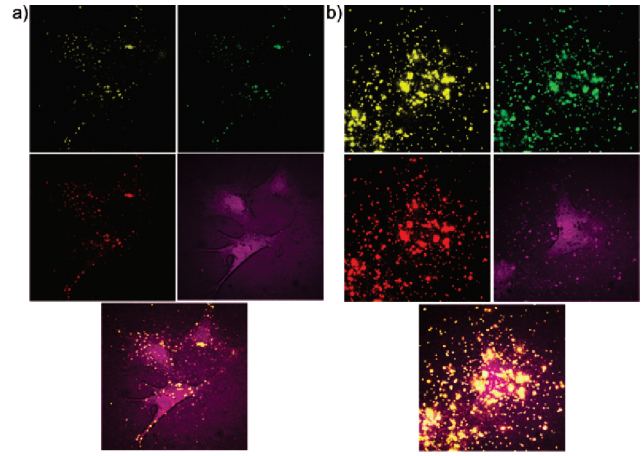

Figure 3. Multiphoton images of A549 cancer cells treated with (a) 10^9 Au NRs/mL and (b) 10^9 Au NR-in-shell nanostructures/mL. The yellow, green, red, and magenta colors indicate 3PF (450−600 nm), SHG band (605−625 nm), 2PF (>650 nm), and THG signals, respectively. The merged images from the four signals are shown in the bottom imaging frames of (a) and (b). The field of view is 16 × 16 μm.

and THG (magenta) intensities of A549 cells treated with Au NR-in-shell nanostructures (Figure 3b) displayed more intense multiphoton signals with better contrast than did those treated with Au NRs (Figure 3a). The NRs distributed in the cells appeared as white spots in the merged image. The imaging signals (Figure 3) were greater than those from cells alone (Figure S8a). If A549 cells were treated with higher Au NR concentrations of 3×10^9 particles/mL (Figure S8b), multiphoton signals comparable to those of Au NR-in-shell nanostructures were observed.

In summary, Au NR-in-shell nanostructures have been successfully synthesized and showed their high efficacy in NIR photothermal destruction of cancer cells and multiphoton imaging contrast.

Acknowledgment. We thank the National Science Council, Taiwan, for financial support of this work. This project was also sponsored by the National Health Research Institute of Taiwan under NHRI-EX98-9201EI.

Supporting Information Available: Experimental section, EDX data, MTT assays, ICP analysis, emission spectra, and multiphoton images. This material is available free of charge via the Internet at http://pubs.acs.org.

References

(1) (a) Huang, X.; El-Sayed, I. H.; Qian, W.; El-Sayed, M. A. *J. Am. Chem. Soc.* **2006**, *128*, 2115. (b) Hauck, T. S.; Jennings, T. L.; Yatsenko, T.; Kumaradas, J. C.; Chan, W. C. W. *Adv. Mater.* **2008**, *20*, 3832. (c) Li, J. L.; Day, D.; Gu, M. *Adv. Mater.* **2008**, *20*, 3866. (d) Norman, R. S.; Stone, J. W.; Gole, A.; Murphy, C. J.; Sabo-Attwood, T. L. *Nano Lett.* **2008**, *8*, 302.

(2) (a) Wang, H.; Huff, T. B.; Zweifel, D. A.; He, W.; Low, P. S.; Wei, A.; Cheng, J. X. *Proc. Natl. Acad. Sci. U.S.A.* **2005**, *102*, 15752. (b) Durr, N. J.; Larson, T.; Smith, D. K.; Korgel, B. A.; Sokolov, K.; Ben-Yakar, A. *Nano Lett.* **2007**, *7*, 941.

(3) (a) Liu, M.; Guyot-Sionnest, P. *J. Phys. Chem. B* **2004**, *108*, 5882. (b) Xiang, Y.; Wu, X.; Liu, D.; Li, Z.; Chu, W.; Feng, L.; Zhang, K.; Zhou, W.; Xie, S. *Langmuir* **2008**, *24*, 3465.

(4) Zijlstra, P.; Bullen, C.; Chon, J. W. M.; Gu, M. *J. Phys. Chem. B* **2006**, *110*, 19315.

(5) Hu, K. W.; Huang, C. C.; Hwu, J. R.; Su, W. C.; Shieh, D. B.; Yeh, C. S. *Chem.—Eur. J.* **2008**, *14*, 2956.

(6) *CRC Handbook of Chemistry and Physics*, 79th ed.; Lide, D.R., Ed.; CRC Press, Boca Raton, FL, 1998; pp 12−191.

(7) (a) Sun, C. K.; Chu, S. W.; Chen, S. Y.; Tsai, T. H.; Liu, T. M.; Lin, C. Y.; Tsai, H. J. *J. Struct. Biol.* **2004**, *147*, 19. (b) Tai, S. P.; Lee, W. J.; Shieh, D. B.; Wu, P. C.; Huang, H. Y.; Yu, C. H.; Sun, C. K. *Opt. Express* **2006**, *14*, 6178.

JA9062772